J Neurophysiol 105: 1918–1931, 2011.
First published February 23, 2011; doi:10.1152/jn.00953.2010.

Responses of developing pedunculopontine neurons to glutamate receptor agonists

Christen Simon, Abdallah Hayar, and Edgar Garcia-Rill
Center for Translational Neuroscience, Department of Neurobiology and Developmental Sciences, University of Arkansas for Medical Sciences, Little Rock, Arkansas

Submitted 3 November 2010; accepted in final form 16 February 2011

Simon C, Hayar A, Garcia-Rill E. Responses of developing pedunculopontine neurons to glutamate receptor agonists. *J Neurophysiol* 105: 1918–1931, 2011. First published February 23, 2011; doi:10.1152/jn.00953.2010.—The pedunculopontine nucleus (PPN) is involved in the generation and maintenance of waking and rapid eye movement (REM) sleep, forming part of the reticular activating system. The PPN receives glutamatergic afferents from other mesopontine nuclei, and glutamatergic input is believed to be involved in the generation of arousal states. We tested the hypothesis that, from postnatal *days 9* to *17* in the rat, there are developmental changes in the glutamate receptor subtypes that contribute to the responses of PPN neurons. Whole cell patch-clamp recordings were conducted using brainstem slices from 9- to 17-day-old rats. All cells (types I, II, and III; randomly selected or thalamic-projecting) responded to bath application of the glutamate receptor agonists *N*-methyl-D-aspartic acid (NMDA) and kainic acid (KA). A developmental decrease in the contribution of the NMDA receptor and developmental increase in the contribution of the KA receptor was observed following electrical stimulation-induced glutamate input. These changes were also observed following bath application in different cell types (randomly selected vs. thalamic-projecting). KA bath application produced an increase in the paired-pulse ratio (PPR) and a decrease in the frequency of miniature excitatory postsynaptic currents (mEPSCs), suggesting that presynaptic KA autoreceptors may decrease the probability of synaptic glutamate input. In contrast, NMDA application produced no changes in the PPR or mEPSCs. Changes in glutamatergic excitability of PPN cell types could underlie the developmental decrease in REM sleep.

arousal; kainic acid; *N*-methyl-D-aspartic acid; pedunculopontine nucleus; rapid eye movement sleep

IN HUMANS, RAPID EYE MOVEMENT (REM) sleep decreases from ~8 h in the newborn to 1 h in the adult (Roffwarg et al. 1966). A similar decrease in REM sleep occurs in the rat during postnatal *days 10-30* (Jouvet-Mounier et al. 1970), with the majority of changes occurring between 10 and 15 days (Garcia-Rill et al. 2008). A number of developmental changes, such as a decrease in electrical coupling, have been observed during this transition period in brainstem nuclei that control arousal states (Garcia-Rill et al. 2008). The pedunculopontine nucleus (PPN) is one of these nuclei, forming part of the reticular activating system (RAS), and is directly involved in generating the activated states of waking and REM sleep (Steriade and McCarley 1990). PPN neurons increase their firing during waking and REM sleep but decrease their firing during slow-wave sleep (SWS) (Datta and Siwek 2002; Steriade et al. 1990). Some PPN neurons fire at the highest frequency only during REM sleep (REM-on), others during both waking and REM sleep (Wake/REM-on), and a third group at the same frequency during waking, REM, and SWS (state-independent) (Datta and Siwek 2002). Stimulation of the PPN potentiates the appearance of fast (20–40 Hz) oscillations in the cortical EEG (Steriade et al. 1991); these fast oscillations are observed during waking and REM sleep but not SWS. Efferent targets of the PPN include the nonspecific intralaminar thalamic (ILT) parafascicular nucleus (Pf) (Capozzo et al. 2003; Semba and Fibiger 1992). The Pf, in turn, sends diffuse projections to the cortex (Van der Werf et al. 2002). The nonspecific thalamic system is thought to allow sensory input to access the machinery that generates conscious experience, which is characterized by the thalamocortical 40-Hz rhythm (Llinas and Ribary 2001).

The PPN is composed of separate populations of cholinergic, glutamatergic, and GABAergic neurons (Wang and Morales 2009) and contains three cell types distinguished by their intrinsic membrane properties. Type I neurons have Ca^{2+}-dependent low-threshold spikes (LTS) and are noncholinergic; type II neurons have a K^+-mediated potassium A current (I_A), and two-thirds are cholinergic; type III neurons have both LTS current and I_A, and one-third are cholinergic (Kamondi et al. 1992; Leonard and Llinas 1990). Sodium-dependent membrane oscillations in type I (L-type channel-dependent) and calcium-dependent high-threshold oscillations in types II and III (N-type channel-dependent) cells have been reported (Takakusaki and Kitai 1997). However, regardless of cell type, almost all PPN neurons can fire at gamma-band frequency, but no higher, when subjected to depolarizing current steps (Simon et al. 2010). This property was proposed to be due to the intrinsic membrane properties of PPN neurons.

The main inputs to the PPN are cholinergic, GABAergic, and glutamatergic, with considerable serotonergic and noradrenergic modulation (Garcia-Rill et al. 2008). Microinjection of glutamate into the PPN of the freely moving adult rat increased waking and REM sleep (Datta et al. 2001b). In contrast, injections of the glutamate receptor agonist, *N*-methyl-D-aspartic acid (NMDA), specifically increased waking (Datta et al. 2001a), whereas injections of the glutamate receptor agonist, kainate (KA), specifically increased REM sleep (Datta 2002). Antagonists of the glutamate receptor α-amino-3-hydroxy-5-methylisoxazole-4-propionic acid (AMPA) or of metabotropic glutamate receptors (mGluR) had no effect on waking or REM sleep (Datta et al. 2002). Furthermore, intracellular recordings in PPN brainstem slices have demonstrated a developmental decrease in the responses of type II cholinergic cells to NMDA and an increase in their response to KA (Kobayashi et al. 2004b).

Address for reprint requests and other correspondence: E. Garcia-Rill, Center for Translational Neuroscience, Dept. of Neurobiology and Developmental Sciences, Univ. of Arkansas for Medical Sciences, Slot 847, 4301 West Markham St., Little Rock, AR 72205 (e-mail: GarciaRillEdgar@uams.edu).

The effects of cholinergic agonists were described in PPN thalamic-projecting and randomly recorded PPN neurons (Good et al. 2007; Ye et al. 2010). A larger percentage of PPN thalamic-projection neurons were found to be inhibited by the nonspecific cholinergic agonist carbachol (CAR) and to have LTS. Differential glutamatergic responsiveness may also be present in PPN thalamic-projecting neurons, which could be critical for the generation of thalamocortical oscillations during arousal states.

We tested the hypothesis that, from postnatal *days 9* to *17* in the rat, there are developmental changes in the glutamate receptor subtypes that contribute to the responses of PPN neurons. Changes in glutamatergic excitability of PPN cell types (REM-on vs. Wake/REM-on; thalamic-projecting vs. randomly recorded; types I, II, and III) could underlie the developmental decrease in REM sleep. To test this hypothesis, we used whole cell patch-clamp recordings and retrograde labeling to determine the responses of PPN neurons to glutamate or glutamate receptor agonists, which could indicate populations of putative REM-on and Wake/REM-on neurons. Furthermore, we analyzed the effects of glutamate receptor agonists on paired-pulse facilitation (PPF) and miniature excitatory postsynaptic currents (mEPSCs) to determine whether there are functional presynaptic glutamate autoreceptors in the glutamatergic afferents to PPN that could modulate the release of excitatory neurotransmitters.

METHODS

Retrograde labeling of PPN thalamic-projecting neurons. Pups aged 7–15 days from adult timed-pregnant Sprague-Dawley rats (280–350 g) were anesthetized with ketamine (65 mg/kg ip) until tail-pinch reflexes were absent. Retrograde labeling of PPN neurons was performed using a Picospritzer (Parker Hannifin) by pressure injection of ~4 μl of 0.02- to 0.2-μm-diameter green fluorescent latex microsphere beads (Lumafluor, Durham, NC) into the thalamus, using a glass pipette with approximately 60- to 70-μm-tip diameter. The green microspheres showed little diffusion and produced well-defined injection sites. The stereotaxic coordinates of the injection sites were (in mm, relative to bregma): anterioposterior (AP) −2 to −3, lateral (L) +0.5 to +0.8, and dorsoventral (DV) −5.5 to −6.5. The same animals were used to prepare brain slices for patch-clamp recordings 48–72 h after injection. Injection sites for each experiment were confirmed by visualization using a Nikon AZ100 microscope (Nikon Instruments, Melville, NY) and NIS-Elements Advanced Research imaging and analysis software. Only neurons from animals with injection sites within thalamocortical nuclei were included in the statistical analysis. All experimental protocols were approved by the Institutional Animal Care and Use Committee of the University of Arkansas for Medical Sciences and were in agreement with the National Institutes of Health (NIH) guidelines for the care and use of laboratory animals.

Slice preparation. Pups aged 9–17 days (some pups did not receive injections of fluorescent beads and were used for random recordings of PPN neurons) from adult timed-pregnant Sprague-Dawley rats (280–350 g) were anesthetized with ketamine (70 mg/kg im) until tail-pinch reflex was absent. Pups were decapitated, and the brain was rapidly removed and cooled in oxygenated sucrose-artificial cerebrospinal fluid (sucrose-aCSF). The sucrose-aCSF consisted of (in mM): 233.7 sucrose, 26 $NaHCO_3$, 3 KCl, 8 $MgCl_2$, 0.5 $CaCl_2$, 20 glucose, 0.4 ascorbic acid, and 2 sodium pyruvate. Four hundred-micrometer sagittal sections containing the PPN were cut using a Vibratome 1000 Plus with a 900R refrigeration system (Vibratome Instruments, St. Louis, MO). Slices were allowed to equilibrate in aCSF at room temperature for 1 h. The aCSF was composed of (in mM): 117 NaCl, 4.7 KCl, 1.2 $MgSO_4$, 2.5 $CaCl_2$, 1.2 NaH_2PO_4, 24.9 $NaHCO_3$, and 11.5 glucose. Some experiments were performed using Mg^{2+}-free aCSF with the following composition (in mM): 117 NaCl, 4.7 KCl, 2.5 $CaCl_2$, 1.2 NaH_2PO_4, 24.9 $NaHCO_3$, and 20 glucose.

Whole cell patch-clamp recordings. Whole cell recordings were performed using borosilicate glass capillaries pulled on a P-97 puller (Sutter Instrument, Novato, CA) and filled with a solution of (in mM): 124 K-gluconate, 10 HEPES, 10 phosphocreatine (di-Tris), 0.2 EGTA, 4 Mg_2ATP, 0.3 Na_2GTP, and 0.5% Neurobiotin (Vector Laboratories, Burlingame, CA). Osmolarity was adjusted to approximately 270–290 mosM and pH to 7.4. The pipette resistance was 5–10 MΩ. Slices were recorded at 30°C while perfused (1.5 ml/min) with oxygenated (95% O_2-5% CO_2) aCSF in an immersion chamber. No series resistance compensation was performed in this study. Neurons were visualized using an upright microscope (Nikon FN1 with ×40 water immersion lens, X1-2 magnifying turret, and Gibraltar Platform; Nikon Instruments) equipped for epifluorescence and near-infrared differential interference contrast optics. The anatomic location of recorded cells within the PPN was confirmed using a ×4 objective lens before and after recording. PPN thalamic-projecting neurons were identified as containing fluorescent beads under epifluorescence illumination using a Lucifer Yellow filter cube with an excitation filter of 425 nm (Chroma Technology, Bellows Falls, VT). Analog signals were low-pass filtered at 2 kHz using a MultiClamp 700B amplifier and digitized at 5 kHz using Digidata 1440A and pCLAMP 10 software (Molecular Devices, Union City, CA). Drugs were administered to the slice by bath application via a peristaltic pump (Cole-Parmer, Vernon Hills, IL) and a three-way valve system.

To determine the intrinsic membrane properties of cells, depolarizing and hyperpolarizing current [resting membrane potential (RMP) = −60 mV; −180 to 90 pA, 30-pA steps, 500-ms duration] or voltage steps [holding potential (HP) = −60 mV; −120 to −10 mV, 15-mV steps, 500-ms duration] were applied under current-clamp and voltage-clamp configuration. The presence of a I_A was determined by testing whether a significant transient outward current was produced in response to a depolarizing voltage step to −60 or −45 mV, which was preceded by a 500-ms negative voltage step to −120 mV. To test the effects of neuroactive agents, cells were held at −60 mV in voltage-clamp mode, and every 20 s, the membrane potential was held at a hyperpolarized level (HP = −120 mV) for 200 ms to determine changes in input resistance (R_{in}), and then a 500-ms voltage ramp from −120 to −40 mV was applied to test the current-voltage relationship of the activated currents. For recording electrically evoked EPSCs, spontaneous EPSCs (sEPSCs), mEPSCs, the membrane potential was held at −70 mV to prevent the generation of action potentials. Furthermore, for recording electrically evoked EPSCs, a hyperpolarizing step from −70 to −120 was applied every 10 s to determine changes in R_{in}. These methods have been published (Heister et al. 2009; Ye et al. 2010).

Electrical stimulation. To evoke EPSCs, electrical stimulation was applied using a bipolar tungsten microelectrode driven by a constant current stimulus isolation unit (Digitimer, Hertfordshire, England). The stimulation electrode (200-kΩ resistance, 50-μm intertip distance) was placed in the PPN, 50–200 μm away from the recorded neurons. Paired-pulse stimuli were delivered at 50-ms intervals every 10 s. Pulse duration was 0.1 ms, and stimulation voltage was adjusted to evoke a consistent response with no failure rate (1.5–1.7 times threshold), as described previously (Heister et al. 2009; Ye et al. 2010).

Drug application. Bath-applied drugs were administered to the slice via a peristaltic pump (Cole-Parmer) and a three-way valve system such that solutions reached the slice 1.5 min after the start of application. Drugs used in this study included the nonspecific cholinergic receptor agonist CAR (30 μM), the glutamate receptor agonists KA (1 μM) and NMDA (4 μM), the sodium channel blocker tetrodotoxin citrate (TTX; 1 μM), the selective NMDA receptor antagonist 2-amino-5-phosphonovaleric acid (APV; 50 μM), the KA receptor

antagonist 6-cyano-7-nitroquinoxaline-2,3-dione (CNQX; 10 μM), the $GABA_A$ receptor antagonist gabazine (GBZ; 10 μM), the glycine receptor antagonist strychnine (STR; 10 μM), and the nicotinic ACh receptor antagonist mecamylamine (MEC; 10 μM). All drugs were purchased from Sigma (St. Louis, MO) except TTX, which was purchased from Tocris Bioscience (Ellisville, MO).

Data analysis. Data analysis was performed as previously reported (Heister et al. 2009; Ye et al. 2010). Off-line analyses were performed using Clampfit 10 software (Molecular Devices). Only cells with action potential amplitudes higher than 45 mV and RMP more negative than −45 mV were included in these analyses. Analysis was conducted using paired Student's *t*-tests and one-way ANOVAs with OriginPro 8.0 software (OriginLab, Northampton, MA). For spontaneous and miniature EPSC studies, the amplitude and inter-EPSC intervals were analyzed using Mini Analysis software (Synaptosoft, Decatur, GA). A Kolmogorov-Smirnov test (K-S test; Clampfit 10) was used to compare the preceding parameters. The amplitude and half-width duration of evoked EPSCs were determined using Clampfit 10 and were further analyzed using Origin 8.0. Paired-pulse ratio (PPR) was also analyzed using OriginPro 8.0. Differences were considered significant at values of $P \leq 0.05$. All results are presented as means ± SE.

Histology. After recordings, slices were fixed overnight in 4% paraformaldehyde and then stored in phosphate-buffered saline for further immunolabeling. Goat polyclonal anti-biotin conjugated to Cy5 [United States Biological (USBio), Swampscott, MA] was used to identify the Neurobiotin in the recorded neurons. Cells were identified using a Nikon confocal fluorescence microscope, and images were taken using the software NIS-Elements.

RESULTS

Location of injection sites and recorded neurons. In some experiments, fluorescent beads were injected into the ILT, which includes the medial, mediodorsal, centromedian, and Pf nuclei. Most injections were ~0.5 mm in diameter in a teardrop shape spreading dorsally along the injection pipette (Fig. 1*A*). All recording sites were located within the PPN as determined using a ×4 objective lens before and after recording (Fig. 1*B*). Thalamic-projecting PPN neurons labeled with fluorescent beads were identified using epifluorescence via a ×40 objective (Fig. 1*C*). Neurobiotin was included in the intracellular pipette solution to label the recorded neurons for further identification (Fig. 1*D*). Overlay of Fig. 1, *C* and *D* (Fig. 1*E*), shows the recorded PPN thalamic-projecting neuron.

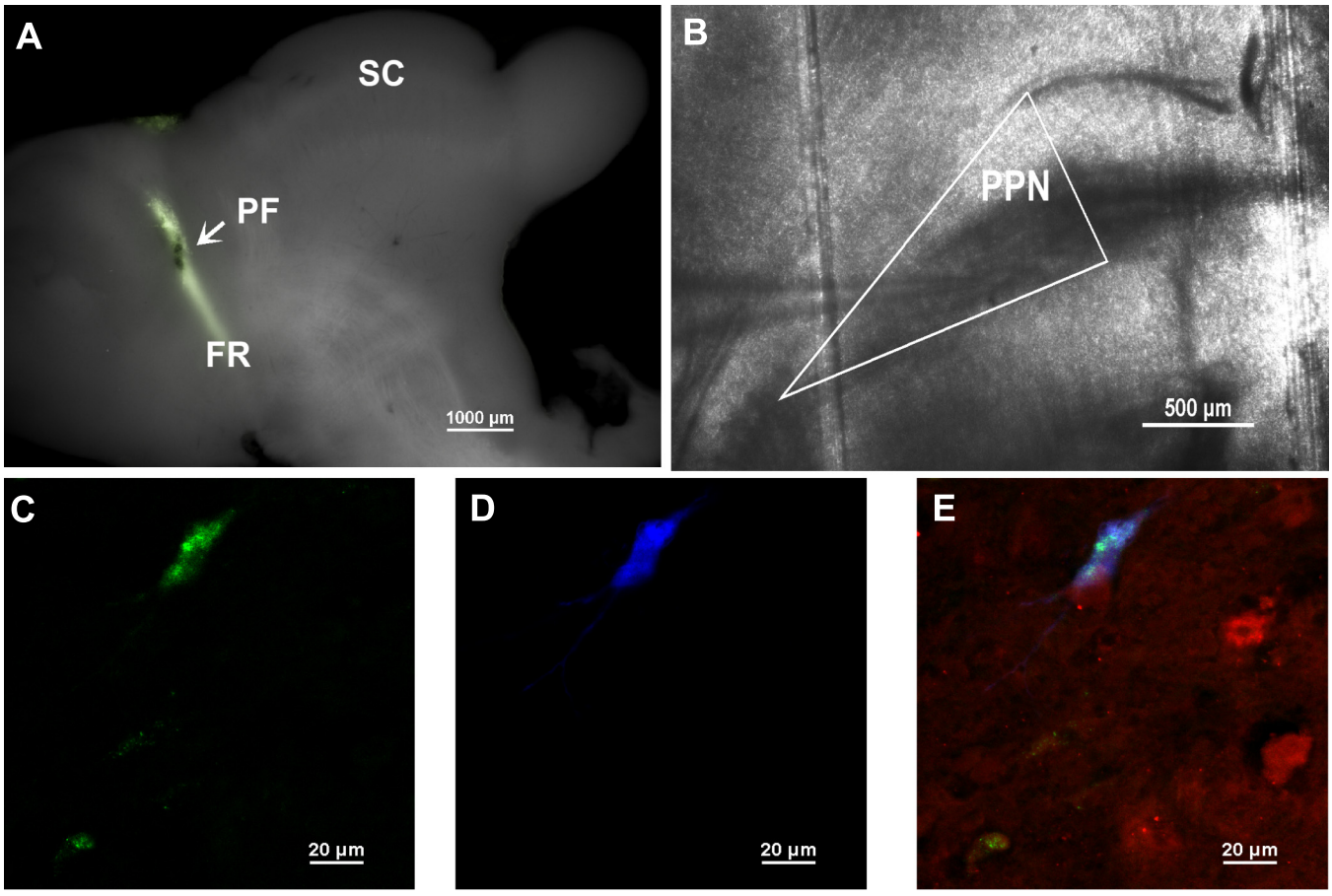

Fig. 1. Injection and recording sites and labeling of recorded neurons. *A*: fluorescent beads were injected into the thalamus (arrow), which included the parafascicular nucleus (Pf). The Pf is located along the fasciculus retroflexus (FR) fiber tract anterior to the superior colliculus (SC). *B*: the pedunculopontine nucleus (PPN) was located by the wedge-shaped cellular region overlapping the superior cerebellar peduncle. The boundary of the PPN (white line) and the placement of the whole cell patch-clamp electrode are shown. *C*: after 48–72 h, injection of fluorescent beads into the thalamus produced labeling in PPN cells. Cells containing beads (green dots) were assumed to be PPN thalamic-projecting neurons that projected to thalamic nuclei. Note labeled cells at *top* and *bottom left*. *D*: to identify neurons following recording, Neurobiotin was included in the pipette solution and was immunocytochemically labeled (blue label) following recording. The PPN thalamic-projection neuron at *top* was also the recorded cell (Neurobiotin; blue label). *E*: brain nitric oxide synthase (bNOS) immunocytochemical labeling (red label) revealed that the recorded cell was not cholinergic (although a cholinergic cell was located next to it). Other cholinergic neurons are shown at *right* and *bottom*. Overlay of *C* and *D* showing that the recorded cell was labeled with fluorescent beads but not bNOS-positive.

Properties of the recorded neurons. In this study, a total of 182 PPN neurons were recorded: 31% (n = 56/182) were classified as type I, 38% (n = 69/182) as type II, 26% (n = 47/182) as type III, and 5% (n = 10/182) had neither LTS current nor I_A and were classified as type IV (Kamondi et al. 1992; Leonard and Llinas 1990). Of the 182 PPN neurons recorded, 43 were labeled with fluorescent beads and, of these, 30% (n = 13/43) were type I, 44% (n = 19/43) were type II, 23% (n = 10/43) were type III, and 2% (n = 1/43) were type IV. These distributions across several subtypes are consistent with our results (Ye et al. 2010). We first determined the responses of these neurons using exogenous (bath) application of glutamate receptor agonists, followed by electrical stimulation to record evoked EPSCs, and we also recorded glutamate-elicited sEPSCs. Then, direct effects on randomly recorded and thalamic-projecting neurons were determined by bath application of glutamate receptor agonists with TTX. Finally, the presence of presynaptic glutamate receptors was also determined using PPR and analyzing mEPSCs.

Postsynaptic responses of PPN neurons. The glutamate receptor agonists NMDA and KA were bath-applied to 43 randomly recorded (animals were not injected with fluorescent beads) PPN neurons, and the responses were recorded in voltage-clamp mode (HP = −60 mV). At RMP, the NMDA receptor exhibits a Mg^{2+} blockade, which is removed by membrane depolarization (Hille 2001; Von Bohlen und Halbach and Dermietzel 2006). Therefore, slices were bathed in Mg^{2+}-free aCSF to observe the full response to NMDA. All PPN neurons responded to bath application of NMDA or KA with an inward current and a decrease in R_{in} (Fig. 2, *A* and *B*).

Cells were divided into three age groups for further analysis: 9–11 days (n = 13), 12–14 days (n = 17), and 15–17 days (n = 13). Consistent with previous results (Kobayashi et al. 2004b), we observed a developmental decrease in response to NMDA [Fig. 2*C*; degrees of freedom (df) = 42, F = 4.00, $P < 0.05$] and a small developmental increase in response to KA (df = 42, F = 3.21, $P < 0.05$). These changes were not due to a developmental change in R_{in} (Fig. 2*D*; df = 42, F =

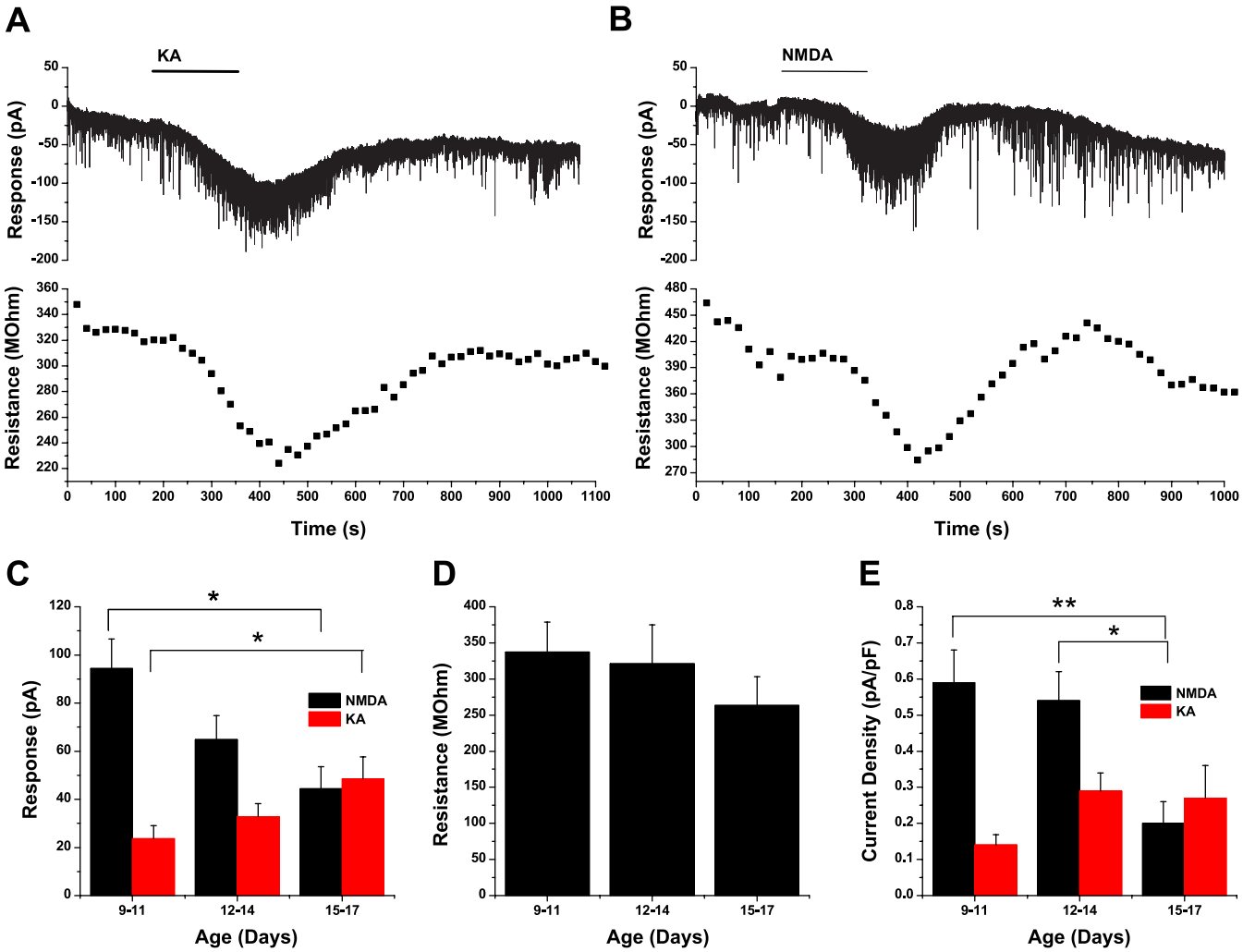

Fig. 2. Responses of PPN neurons to application of glutamate receptor agonists. *A*: kainate (KA) was bath-applied to observe effects on the recorded neurons. The response to KA was marked by a decrease in input resistance (R_{in}), which decreased by 33%, as shown in the graph plotting resistance in megohms over time (seconds). *B*: the response to *N*-methyl-D-aspartic acid (NMDA) was also marked by a decrease in R_{in}, which decreased by 38%, as shown in the graph plotting resistance in megohms over time (seconds). *C*: a significant developmental decrease in response to NMDA and developmental increase in response to KA was observed between 9 and 11 and between 15 and 17 days ($P < 0.05$). *D*: these developmental changes were not a result of changes in R_{in} ($P > 0.05$) across the 3 age groups of 9–11, 12–14, and 15–17 days. *E*: the developmental decrease in response to NMDA was still observed after normalizing for cell capacitance ($P < 0.01$), but no developmental changes were observed following KA (*$P < 0.05$, **$P < 0.01$).

0.52, $P > 0.05$). Since cholinergic cells in the PPN increase in size during this developmental period (Kobayashi et al. 2004a), the current response was normalized to the capacitance to determine the current density (Fig. 2*E*). A developmental decrease was still observed in response to NMDA (df = 42, $F = 6.13$, $P < 0.01$), and no developmental changes were observed in response to KA (df = 42, $F = 2.23$, $P > 0.05$), although there did appear to be an increasing trend.

The experiment described above (shown in Fig. 2) used exogenous (bath) application of glutamate receptor agonists to examine the responses mediated by ionotropic glutamate receptors. To confirm these results, stimulating electrodes were placed in the PPN, and local axons were activated; this experiment would reveal whether a developmental change is present in synaptic glutamate responses. These experiments were performed on random PPN neurons (not thalamic-projecting), and Mg^{2+}-free aCSF was used. The $GABA_A$ and glycine receptor antagonists, GBZ and STR, respectively, were added to block fast inhibitory neurotransmission and observe only the responses to excitatory neurotransmitters. APV was then added to block NMDA receptors followed by CNQX to block AMPA/KA receptors. Figure 3, *A* and *B*, shows the response of a neuron in a slice from a 10-day-old rat. Application of APV blocked a large portion of the stimulation-induced response. The same experiment was performed in a neuron in a slice from a 16-day-old rat (Fig. 4, *C* and *D*). Application of APV did not greatly reduce the response, but the response was considerably reduced following application of CNQX. Averaging the amplitude of the response for all of the recordings ($n = 21$; Fig. 3*E*) shows that between 9 and 11 days ($n = 11$) and 15 and 17 days ($n = 10$), the percentage of the response amplitude blocked by application of APV decreased, whereas the percentage of the response amplitude blocked by CNQX increased (df = 19, $t = 2.77$, $P < 0.01$). This was also

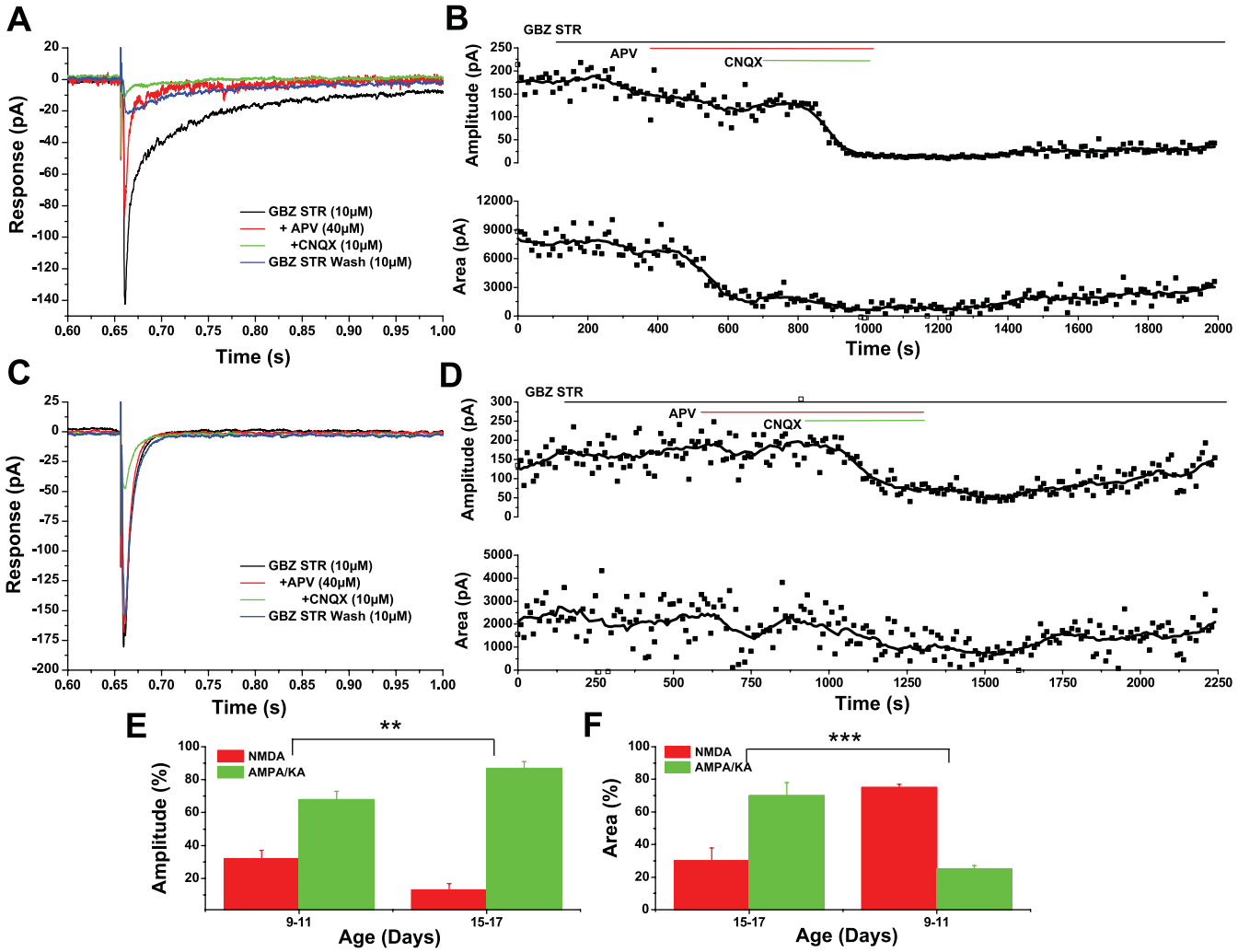

Fig. 3. Antagonist effects on locally evoked glutamate responses. Electrodes were placed in the PPN 50–200 μm away from the recorded neuron. *A*: in a neuron from a 10-day-old rat, application of 2-amino-5-phosphonovaleric acid (APV; red record) greatly decreased the excitatory postsynaptic current (EPSC) compared with gabazine (GBZ) and strychnine (STR) alone (black record). Application of 6-cyano-7-nitroquinoxaline-2,3-dione (CNQX; green record) blocked the remainder of the response. *B*: amplitude (*top*) and area (*bottom*) of EPSCs during the entire recording. *C*: in a neuron from a 16-day-old rat, application of APV (red record) decreased the EPSC only slightly compared with GBZ and STR alone (black record). Application of CNQX (green record) blocked most of the remainder of the response. *D*: amplitude (*top*) and area (*bottom*) of the EPSC during the entire recording. *E*: average percentage of the EPSC amplitude blocked by application of APV (red bars) vs. CNQX (green bars) in all of the recorded neurons across development. Between 9 and 11 and between 15 and 17 days, CNQX blocked a significantly higher percentage of the EPSC amplitude, and APV blocked a significantly lower percentage ($P < 0.01$). *F*: CNQX also blocked a significantly higher percentage of the EPSC area, and APV blocked a significantly lower percentage (**$P < 0.01$, ***$P < 0.001$).

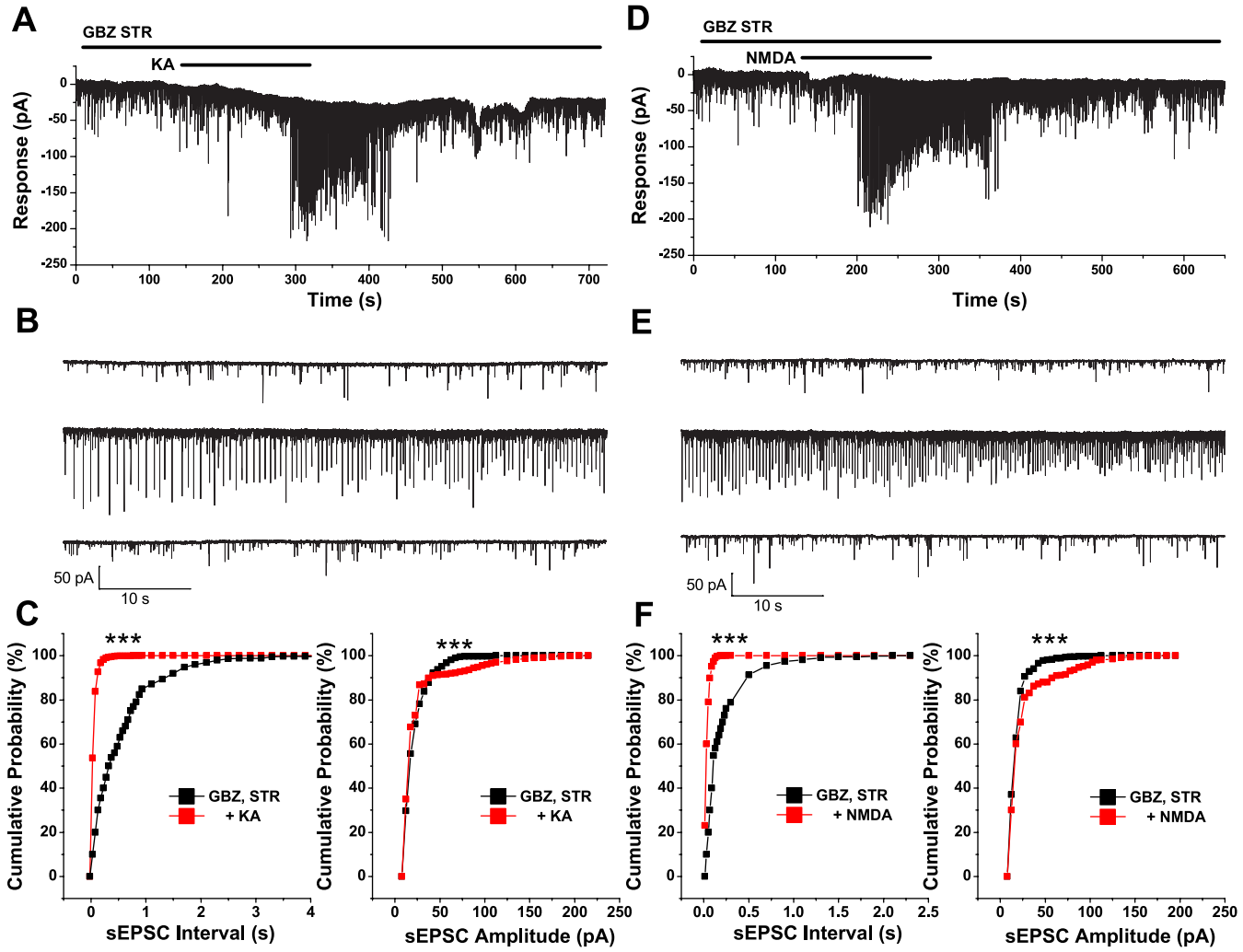

Fig. 4. Effects of glutamate receptor agonists on spontaneous EPSCs (sEPSCs). *A*: representative recording of a cell with an increase in sEPSCs following application of KA in the presence of GBZ and STR. *B*: 1-min segments taken from the recording in *A* showing sEPSCs during GBZ and STR (*top* record), addition of KA (*middle* record), and following wash with GBZ and STR (*bottom* record). *C*: cumulative probability distributions of the inter-sEPSC interval (*left*) and sEPSC amplitude (*right*). Application of KA significantly decreased the inter-sEPSC interval ($P < 0.001$) and increased the amplitude of sEPSCs ($P < 0.001$) in this neuron. *D*: representative recording of a cell that had an increase in sEPSCs following application of NMDA in the presence of GBZ and STR. *E*: 1-min segments taken from the recording in *D* showing sEPSCs during GBZ and STR (*top* record), addition of NMDA (*middle* record), and following wash with GBZ and STR (*bottom* record). *F*: cumulative probability distributions of the inter-sEPSC interval (*left*) and sEPSC amplitude (*right*). Application of NMDA significantly decreased the inter-sEPSC interval ($P < 0.001$) and increased the amplitude of sEPSCs (***$P < 0.001$) in this neuron.

observed when measuring the response area (df = 19, $t = 5.97$, $P < 0.001$).

The effects of glutamate receptor agonists on sEPSCs were also tested in randomly recorded PPN neurons. An increase in spontaneous synaptic activity would indicate that KA or NMDA have excited neurons that project to the recorded neuron. These experiments were performed in the presence of GBZ and STR to block inhibitory neurotransmission and using normal Mg^{2+} aCSF. Application of KA increased the frequency of sEPSCs in 60% (n = 9/15) and increased the amplitude of sEPSCs in 33% (5/15) of the neurons tested (Fig. 4, *A* and *B*; K-S test, $P < 0.05$). No effects were observed in the remaining neurons. Figure 4*C* shows cumulative probability distributions of the inter-sEPSC interval (*left*) and sEPSC amplitude (*right*). The leftward shift in the cumulative probability distribution of inter-sEPSC interval indicates a decrease in the inter-sEPSC interval (increase in frequency) following application of KA (K-S test, $P < 0.001$). The slight rightward shift in the cumulative probability distribution of sEPSC amplitude indicates an increase in sEPSC amplitude following application of KA (K-S test, $P < 0.001$). KA increased the number of both small and large sEPSCs, thus having an effect across the entire range of amplitude distribution.

NMDA produced an increase in sEPSC frequency in 59% (n = 10/17) and increase in amplitude in 35% (6/17) of the recorded neurons (Fig. 4, *D* and *E*; K-S test, $P < 0.05$). In the other 41% (n = 7/17), no changes were observed. Figure 4*F* shows cumulative probability distributions of the inter-sEPSC interval (*left*) and sEPSC amplitude (*right*). The leftward shift in the cumulative probability distribution of the inter-sEPSC interval indicates a decrease in the inter-sEPSC interval (increase in frequency) following application of NMDA (K-S test, $P < 0.001$). A slight rightward shift in the cumulative probability distribution of sEPSC amplitude indicates an increase in sEPSC amplitude following application of NMDA (K-S test, $P < 0.001$). NMDA increased the number of both small and

large sEPSCs, thus also having an effect across the entire range of amplitude distribution.

Direct postsynaptic responses of PPN neurons to glutamate receptor agonists. To determine the direct effect of NMDA and KA on PPN neurons, NMDA was bath-applied to 51 and KA to 58 randomly recorded (animals were not injected with fluorescent beads) PPN neurons in the presence of TTX to block action potential generation. Responses were recorded in voltage-clamp mode (HP = −60 mV). Slices were bathed in Mg^{2+}-free aCSF to observe the full response to NMDA. All PPN neurons responded to bath application of NMDA or KA with an inward current and decrease in R_{in} (Fig. 5, *A* and *B*).

Cells were divided into three age groups for further analysis: 9–11 days (NMDA $n = 15$, KA $n = 15$), 12–14 days (NMDA $n = 23$, KA $n = 25$), and 15–17 days (NMDA $n = 13$, KA $n = 18$). Consistent with the above experiments (Figs. 2 and 3), we observed a developmental decrease in response to NMDA (Fig. 5*C*; df = 50, $F = 4.45$, $P < 0.05$). However, although it appeared there was a small developmental increase in response to KA, this was not statistically significant (df = 57, $F = 0.50$, $P > 0.05$). These changes were not due to a developmental change in R_{in} (Fig. 2*D*; df = 48, $F = 0.18$, $P > 0.05$). Following normalization of the current response to capacitance to determine the current density (Fig. 5*E*), a developmental decrease was still observed in response to NMDA (df = 50, $F = 5.01$, $P < 0.01$), and no developmental changes were observed in response to KA (df = 57, $F = 0.04$, $P > 0.05$).

NMDA and KA were also bath-applied to PPN thalamic-projecting neurons ($n = 43$), which were identified as described above. TTX was used to examine the direct effects of glutamate receptor agonists. Figure 6, *A* and *B*, shows the response of a neuron from a 13-day-old rat to application of NMDA and KA. All thalamic-projecting neurons responded to application of NMDA and KA with an inward current and decrease in R_{in}.

Cells were divided into the same three age groups described above: 9–11 days ($n = 13$), 12–14 days ($n = 21$), and 15–17

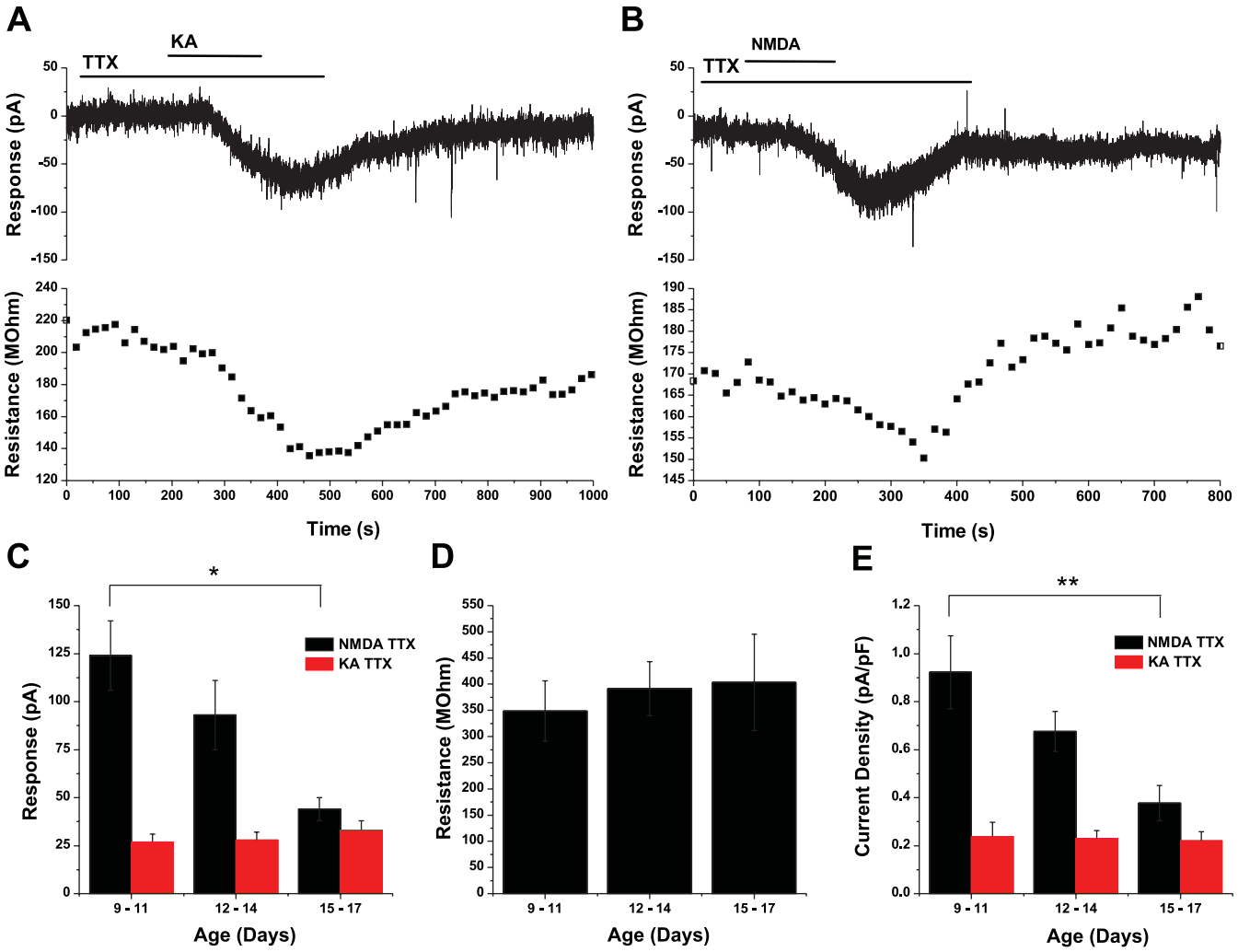

Fig. 5. Direct effect of PPN neurons to application of glutamate receptor agonists. *A*: KA was applied in the presence of TTX to observe the direct effects of KA on this neuron. The response to KA was marked by a decrease in R_{in}, which decreased by 33%, as shown in the graph plotting resistance in megohms over time (seconds). *B*: NMDA was applied in the presence of the sodium channel blocker TTX to observe the direct effects by NMDA on this neuron. The response to NMDA was marked by a decrease in R_{in}, which decreased by 12%, as shown in the graph plotting resistance in megohms over time (seconds). *C*: a significant developmental decrease in response to NMDA was observed between 9 and 11 and between 15 and 17 days ($P < 0.05$), but no significant developmental changes were observed in response to KA ($P > 0.05$). *D*: these developmental changes were not a result of changes in R_{in} ($P > 0.05$) across the 3 age groups of 9–11, 12–14, and 15–17 days. *E*: the developmental decrease in response to NMDA was still observed after normalizing the cell area ($P < 0.01$), and no developmental changes were observed following KA (*$P < 0.05$, **$P < 0.01$).

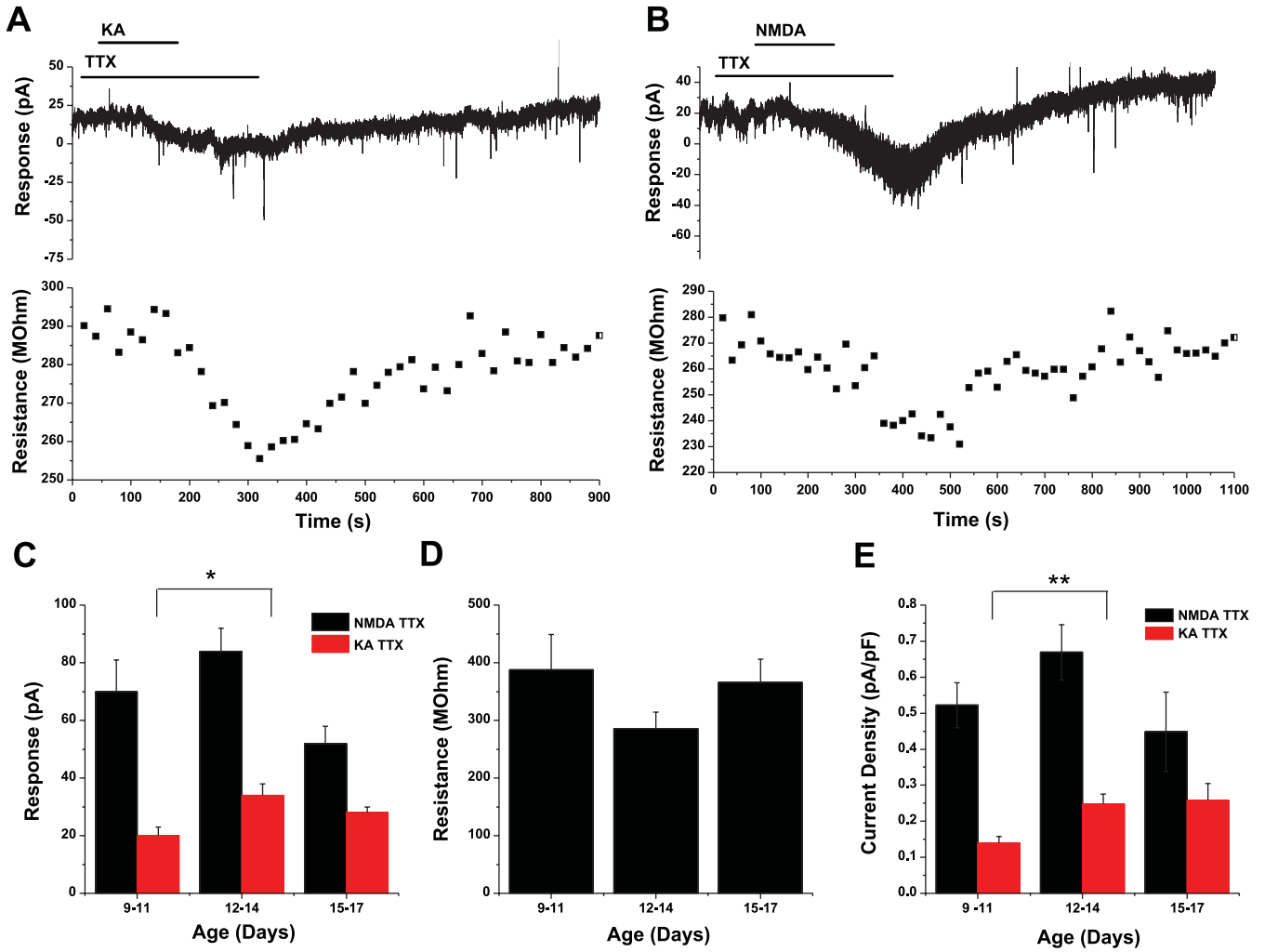

Fig. 6. Direct effect of PPN thalamic-projecting neurons to glutamate receptor agonists. *A*: KA was applied in the presence of TTX to observe the direct effect on this neuron. The response to KA was marked by a decrease in R_{in}, which decreased by 12%, as shown in the graph plotting resistance in megohms over time (seconds). *B*: NMDA was applied in the presence of the sodium channel blocker TTX to observe the direct effects on this neuron. The response to NMDA was marked by a decrease in R_{in}, which decreased by 18%, as shown in the graph plotting resistance in megohms over time (seconds). *C*: a significant developmental increase in the response to KA was observed between 9 and 11 and between 12 and 14 days ($P < 0.05$). No significant changes were observed in response to NMDA ($P > 0.05$). *D*: these developmental changes were not the result of changes in R_{in} ($P > 0.05$). *E*: the developmental increase in response to KA was still observed after normalizing the cell area ($P < 0.01$), and no developmental changes were observed following application of NMDA (*$P < 0.05$, **$P < 0.01$).

days ($n = 9$). In thalamic-projecting neurons, we observed no significant change in the response to NMDA (Fig. 6*C*; df = 42, $F = 1.98$, $P > 0.05$). However, there appeared to be a decreasing trend from 12 to 14 to 15 to 17 days. Furthermore, unlike in the randomly recorded cells, a developmental increase in response to KA was observed between 9 and 11 and between 12 and 14 days (df = 41, $F = 3.27$, $P < 0.05$). These changes were not due to variations in R_{in} (Fig. 6*D*; df = 42, $F = 1.67$, $P > 0.05$). Following normalization of the current response to capacitance to determine the current density (Fig. 3*E*), no developmental changes were observed in response to NMDA (df = 42, $F = 1.77$, $P > 0.05$), and a developmental increase was still observed in response to KA (df = 41, $F = 5.30$, $P < 0.01$) between 9 and 11 and between 12 and 14 days.

Presynaptic responses of PPN neurons to glutamate receptor agonists. The PPR (ratio of the 2nd evoked EPSC divided by the 1st) is measured by paired stimulation with a short interstimulus interval (50 ms in this experiment). PPF occurs when, following the response to the 1st stimulus, there is residual calcium in the axon terminal resulting in an increase in the probability of synaptic release following the initial stimulus (Debanne et al. 1996). Binding of agonist to presynaptic receptors, if excitatory, increases the amplitude of the 1st EPSC and decreases the PPR. The opposite effect would occur if the presynaptic receptors are inhibitory. Therefore, a change in the PPR following agonist application is believed to be due to an effect mediated through presynaptic receptors (Debanne et al. 1996). This experiment was performed with normal Mg^{2+} aCSF and in the presence of GBZ and STR to block inhibitory neurotransmission, which removed possible indirect effects that are due to activation of $GABA_A$ and glycine receptors. KA was bath-applied to 16 neurons during paired-pulse stimulation. Figure 7*A* shows an average of 10 recordings in the presence of GBZ and STR (*left*) and during additional application of KA (*right*) to a neuron in a slice from a 12-day-old rat. Application of KA decreased the amplitude of

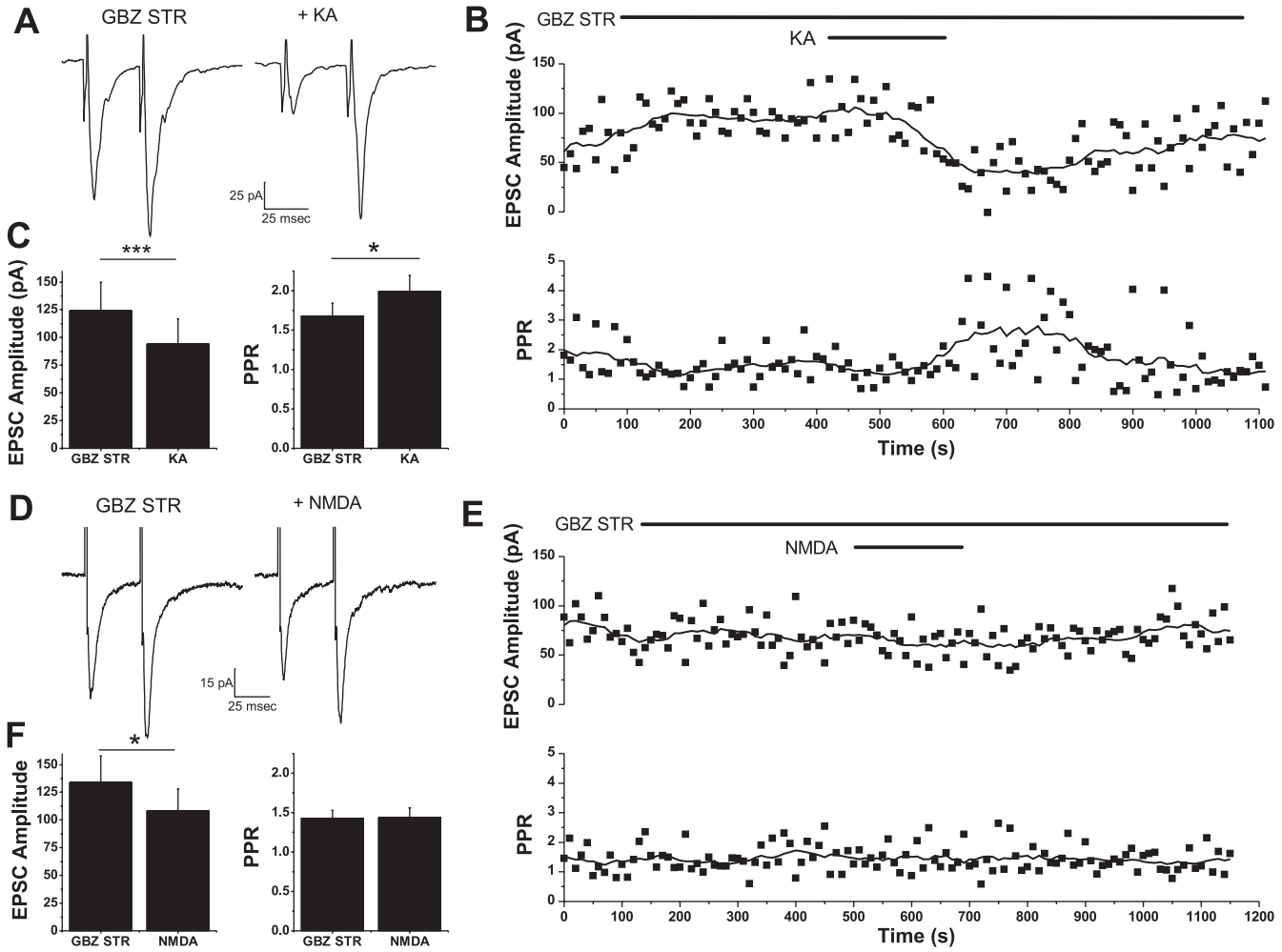

Fig. 7. Paired-pulse ratio (PPR) revealed presynaptic KA receptors. Cells were stimulated twice with an interstimulus interval of 50 ms. *A*: PPF was observed in this neuron during application of GBZ and STR. Application of KA reduced the amplitude of the 1st EPSC without affecting the 2nd EPSC. *B*: application of KA decreased the amplitude of the 1st EPSC (*top*) and increased the PPR (*bottom*). *C*: application of KA significantly decreased the amplitude of the 1st EPSC ($P < 0.001$) and increased the PPR ($P < 0.05$) in all of the recorded neurons. *D*: application of NMDA did not appear to have an effect, as both paired responses were similar before and after NMDA exposure. *E*: amplitude of the 1st EPSC (*top*) and PPR (*bottom*) during the entire recording. Application of NMDA did not change the amplitude of the 1st EPSC or change the PPR. *F*: average change in EPSC amplitude and PPR following GBZ and STR vs. NMDA in all of the recorded neurons. Application of NMDA significantly decreased the amplitude of the 1st EPSC ($P < 0.05$) but did not change the PPR (*$P < 0.05$, ***$P < 0.001$).

the 1st EPSC and increased the PPR in this neuron (Fig. 7*B*), indicating an inhibitory presynaptic effect. Figure 7*C* shows group data from all the recorded neurons ($n = 16$). KA significantly decreased the amplitude of the 1st EPSC (df = 15, $t = 4.24$, $P < 0.001$) and increased the PPR (df = 15, $t = 2.42$, $P < 0.05$).

The effects of NMDA on the PPR were also examined on 17 PPN neurons. Figure 7*D* shows an average of 10 recordings during GBZ and STR and following additional application of NMDA to a neuron in a slice from a 12-day-old rat. NMDA did not appear to change the amplitude of the 1st EPSC or change the PPR (Fig. 7*E*). In group data from all of the recorded neurons ($n = 17$), application of NMDA slightly decreased the amplitude of the 1st EPSC (df = 16, $t = 2.47$, $P < 0.05$) but did not change the PPR (df = 16, $t = 0.12$, $P > 0.05$). In the group data, there was no recovery of EPSC amplitude following wash, indicating that the significant decrease in the amplitude of the 1st EPSC following NMDA compared with GBZ and STR could be due to a slight rundown of the response, which would explain why there was no significant change in the PPR following application of NMDA. Alternatively, this could be due to a small postsynaptic effect on NMDA receptors or a shunting effect due to the decrease in R_{in} in response to NMDA.

The effects of glutamate receptor agonists were also tested on mEPSCs (in the presence of GBZ, STR, and TTX and with normal Mg^{2+} aCSF). Miniature EPSCs are the result of spontaneous release of vesicles from axon terminals. A change in mEPSC frequency following application of agonist would indicate the presence of a presynaptic receptor that modulates release of glutamate. Following application of KA, 53% ($n = 8/15$) of neurons showed a decrease in mEPSC frequency, and 26% (4/15) showed a decrease in mEPSC amplitude (K-S test, $P < 0.05$). No effects were observed in the remaining neurons. Figure 8, *A* and *B*, shows a recording of a neuron in a slice from a 12-day-old rat during application of KA. KA significantly increased the interval of mEPSCs (decreased the frequency) in this neuron (Fig. 8*C*, *left*; K-S test, $P < 0.05$). Application of KA also slightly decreased the amplitude of mEPSCs (Fig. 8*C*, *right*; K-S test, $P < 0.05$).

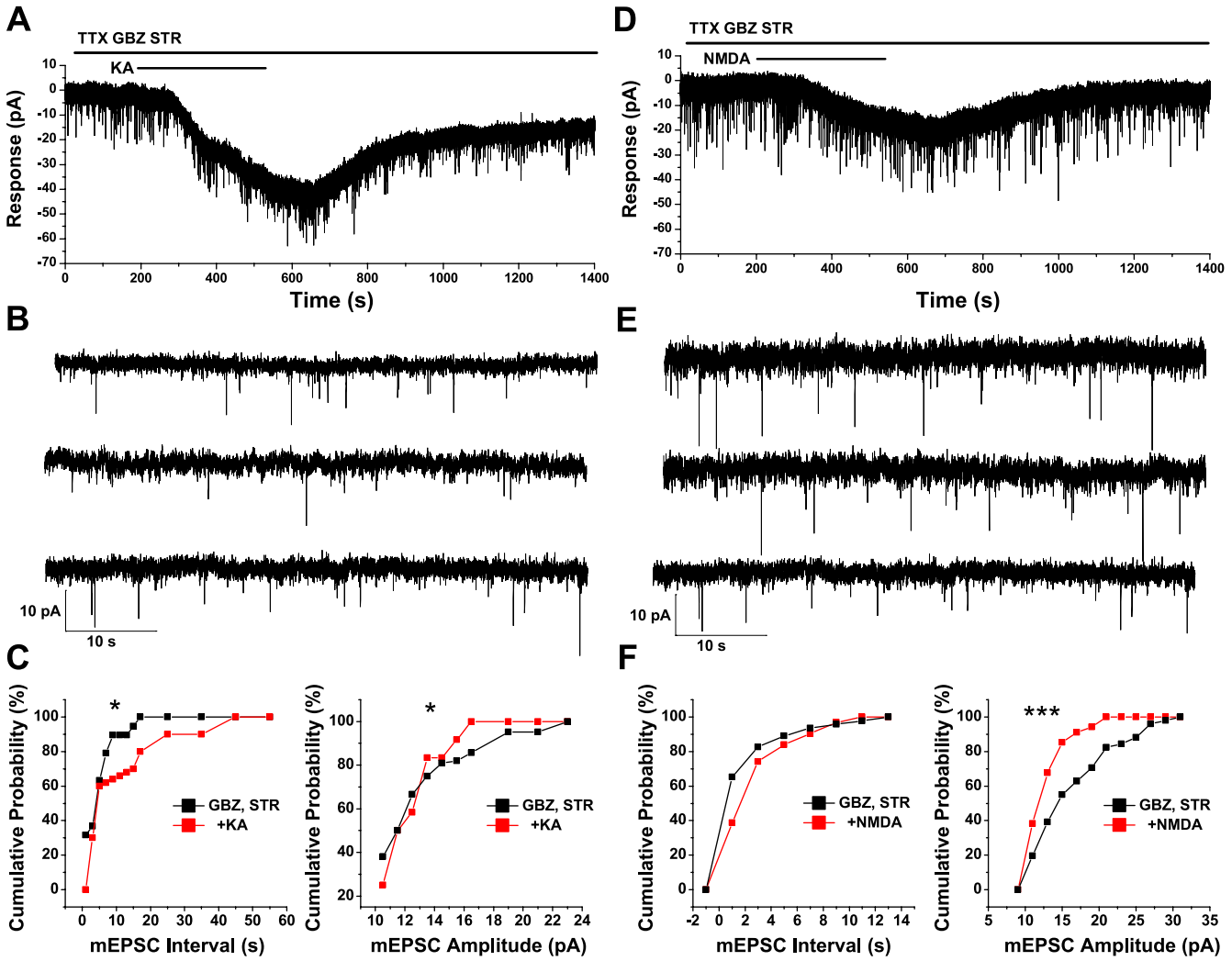

Fig. 8. Effects of glutamate receptor agonists on mEPSCs. *A*: representative recording of a cell that showed a decrease in mEPSCs following application of KA in the presence of GBZ, STR, and TTX. *B*: 1-min segments taken from the recording in *A* showing mEPSCs during GBZ, STR, and TTX (*top* record), addition of KA (*middle* record), and following wash with GBZ, STR, and TTX (*bottom* record). *C*: cumulative probability distributions of the inter-mEPSC interval (*left*) and mEPSC amplitude (*right*). *D*: representative recording of a cell that had no change in mEPSCs following application of NMDA in the presence of GBZ, STR, and TTX. *E*: 1-min segments taken from the recording in *D* showing mEPSCs during GBZ, STR, and TTX (*top* record), addition of NMDA (*middle* record), and following wash with GBZ, STR, and TTX (*bottom* record). *F*: cumulative probability distributions of the inter-mEPSC interval (*left*) and mEPSC amplitude (*right*; $*P < 0.05$, $***P < 0.001$).

The effect of NMDA on mEPSCs was also tested (Fig. 8, *D–F*) to test for functional presynaptic NMDA receptors on glutamatergic terminals. No changes in mEPSC frequency or mEPSC amplitude were observed in all nine neurons tested (K-S test, $P > 0.05$). Figure 8, *E* and *F*, shows a recording of a neuron in a slice from a 12-day-old rat during application of NMDA. No significant change in the inter-mEPSC interval was observed in this neuron (Fig. 8*F*, *left*; K-S test, $P > 0.05$). However, the amplitude of the mEPSCs significantly decreased during application of NMDA in this neuron (Fig. 8*F*, *right*; K-S test, $P < 0.001$), but the amplitude did not recover following a 15-min wash, indicating this decrease could be due to rundown of the response.

It is possible that at least some of the glutamate agonist-induced increase in glutamate input may result from ACh output and the activation of nicotinic receptors on glutamate axon terminals. This possibility was examined particularly in experiments where action potential propagation was not blocked by TTX. Paired-pulse and sEPSC experiments were performed in the presence of the nicotinic receptor antagonist MEC (10 μM), and a significant increase in the PPR was observed following KA (df = 1, $t = 32.61$, $P < 0.05$), but no change was observed following NMDA (df = 2, $t = 1.32$, $P > 0.05$). Furthermore, an increase in sEPSCs following KA (K-S test, $P < 0.001$) and NMDA (K-S test, $P < 0.001$) was observed (results not shown). These results are consistent with those reported (Figs. 4 and 7).

DISCUSSION

This study determined that all PPN neurons (types I, II, and III, randomly recorded or thalamic-projecting) are excited by bath application of the glutamate receptor agonists KA and NMDA. A developmental decrease in response to NMDA was observed following bath application. Local stimulation revealed a developmental decrease in the response mediated by the NMDA receptor and an increase in the response through

the KA receptor. NMDA and KA were also found to decrease the inter-sEPSC interval (increase the frequency), indicating that these agonists excite neurons presynaptic to the recorded neuron. To determine direct responses of PPN neurons, TTX was bath-applied with KA and NMDA to block synaptic transmission. These experiments also revealed a developmental decrease in the response to NMDA specifically in randomly recorded PPN neurons and a developmental increase in the response to KA specifically in thalamic-projecting neurons. To test the function of presynaptic glutamate receptors, the PPR and mEPSCs were measured before and after bath application of agonists. An increase in the PPR and decrease in mEPSCs were also observed following application of KA, but not NMDA, indicating the presence of presynaptic KA receptors modulating excitatory inputs to PPN neurons.

Glutamate receptors are either ionotropic or metabotropic (mGluR). Ionotropic receptors include the KA, NMDA, and AMPA subtypes. mGluRs are G protein-coupled and activate intracellular signaling pathways. KA has traditionally been described as an agonist of KA receptors, directly opening ion channels and changing the membrane potential. However, recent evidence has described metabotropic actions of KA receptors through G protein activation and intracellular signaling cascades (Rodriguez-Moreno and Sihra 2007). KA and AMPA receptors are faster to activate than NMDA receptors and also desensitize relatively quickly. In contrast, NMDA receptors are slower to activate due to the presence of the Mg^{2+} block at RMP and are slower to desensitize than KA and AMPA receptors (Hille 2001; Von Bohlen und Halbach and Dermietzel 2006).

Postsynaptic responses of PPN neurons. The PPN contains three cell types distinguished by their intrinsic membrane properties and is composed of separate populations of glutamatergic, cholinergic, and GABAergic neurons (Kamondi et al. 1992; Leonard and Llinas 1990; Wang and Morales 2009). Our results show that all PPN neurons were excited by glutamate receptor agonists (Fig. 2). In comparison, 73% of PPN thalamic-projecting neurons were inhibited and 13% excited directly by cholinergic input (Ye et al. 2010). A developmental decrease in response to NMDA was observed, which is consistent with our results (Kobayashi et al. 2004b).

Exogenous application of receptor agonists is considered an appropriate way to test the direct effects of neuroactive agents on neurons (Ye et al. 2010). However, local stimulation of nearby axons is a more physiological approach to examine the developmental changes in response to endogenously released neurotransmitters. Glutamate receptor antagonists were added to determine the relative contribution of NMDA receptors vs. KA receptors to the evoked EPSCs (Fig. 3). This experiment revealed significant developmental changes in the relative role of glutamate receptor subtypes in fast excitatory synaptic transmission in the PPN. During development, the response mediated by the NMDA receptor decreased, whereas the response mediated by the KA receptor increased. However, it has yet to be determined whether these changes are a result of modification of receptor number or a change in the affinity of the receptors.

Application of CAR increased the frequency of sEPSCs and spontaneous inhibitory PSCs (sIPSCs), indicating that CAR excites glutamatergic, GABAergic, and/or glycinergic neurons that are presynaptic to PPN thalamic-projecting neurons (Ye et al. 2010). In the present study, we did not test the effects of glutamate receptor agonists on sIPSCs, but we did observe an increase in sEPSCs following application of NMDA or KA in ~60% of the neurons tested (Fig. 4). Therefore, application of these agonists excited neurons that were presynaptic to the recorded PPN neurons. In the other ~40% of neurons recorded, no significant change in sEPSCs was observed. This is possibly a result of cutting presynaptic connections during slice preparation.

Role of glutamate receptor subtypes in the direct postsynaptic responses of PPN neurons. We found that all neurons were excited by bath application of NMDA or KA (Fig. 2). To confirm that these responses were direct, the sodium channel blocker TTX was bath-applied with NMDA and KA (Fig. 5). Furthermore, thalamic-projecting neurons were identified by injecting fluorescent beads into the ILT, and recordings were performed from PPN neurons that contained these beads (Fig. 6). All random and thalamic-projecting neurons responded to NMDA and KA, but different developmental changes were observed in thalamic-projecting neurons vs. randomly recorded neurons. In randomly recorded neurons, a significant developmental decrease was observed in response to NMDA. However, in thalamic-projecting neurons, it appeared that there was a decreasing trend in response to NMDA during development, but this change did not reach significance. Furthermore, unlike in randomly recorded neurons, there was a developmental increase in response to KA from 9 to 11 to 12 to 14 days in thalamic-projecting cells. We have not determined whether this is due to a change in receptor number, sensitivity, or some other mechanism. However, it is likely that changes in the excitability of PPN thalamic-projection neurons would have some effect on their efferent targets and thus on generation or maintenance of waking and REM sleep.

Glutamatergic neurotransmission undergoes many changes during development in other areas of the central nervous system, including the hippocampus. At *day 2*, only NMDA receptors are present at many hippocampal synapses. Since NMDA receptors are blocked at RMP, synaptic release of glutamate does not produce a response in these neurons, and these synapses have been called silent synapses. However, by *day 5*, the number of silent synapses decreases as a result of increased AMPA/KA receptor trafficking to the membrane (Ben-Ari et al. 1997; Pickard et al. 2000). Similar results have been observed in thalamocortical neurons, where silent synapses disappear by *days 8-9* (Isaac et al. 1997). Developmental changes in the amplitude of NMDA receptor-mediated EPSCs, and in the sensitivity of the NMDA receptor, have also been observed. In the cortex, there is little change in the affinity of NMDA receptors to glutamate during development, but a population of neurons exhibits a decreased affinity for glycine in rats between postnatal *days 14* and *28* (Kew et al. 1998). At ferret retinogeniculate synapses, a developmental decrease in the duration and amplitude of NMDA receptor-mediated responses occurs following the first 2 postnatal weeks (Ramoa and McCormick 1994). Furthermore, in the auditory brainstem, the amplitude of NMDA receptor-mediated EPSC decreased from *day 10* to *18* (Steinert et al. 2010). However, at cerebellar mossy fiber-granule cell synapses, the contribution of NMDA receptors vs. non-NMDA receptors to the EPSC was similar at *day 7* and postnatal *days 21* and *40* (Cathala et al. 2000).

Presynaptic glutamate receptors. Presynaptic KA responses have been obtained in the cortex (Campbell et al. 2007), hippocampus (Lauri et al. 2005; Schmitz et al. 2001), globus pallidus (Jin et al. 2006), cerebellum (Delaney and Jahr 2002), and spinal cord (Kerchner et al. 2001; Lu et al. 2005). In the cortex, activation of presynaptic receptors by low concentrations of KA (50–500 nM) facilitated the release of neurotransmitters, whereas a higher concentration (3 μM) was inhibitory (Campbell et al. 2007). Similar concentration-dependent effects have also been observed in the hippocampus (Schmitz et al. 2001). Also in the hippocampus, during the first postnatal week, presynaptic KA receptors inhibited glutamate release through a G protein- and a PKC-dependent pathway (Lauri et al. 2005). Metabotropic effects of presynaptic KA receptors were also observed in the globus pallidus, when activation of presynaptic KA receptors using 1 μM KA inhibited EPSCs and increased the PPF. This effect was blocked by application of G protein or PKC inhibitors (Jin et al. 2006). Furthermore, in dorsal root ganglia, KA (10 μM) decreased spontaneous NMDA receptor-mediated EPSCs in culture, indicating an inhibitory effect.

In the present study, we observed an increase in the PPR (Fig. 7) and a decrease in mEPSCs (Fig. 8) following application of KA, indicating presynaptic inhibition. The finding of cholinergic agonist-increased glutamate input to PPN thalamic-projecting neurons provides a neural substrate for the present results (Ye et al. 2010). It has yet to be determined whether these effects are concentration-dependent or whether presynaptic KA receptors in the PPN have metabotropic actions. Presynaptic NMDA receptors have been observed in the cortex (Li et al. 2008), hippocampus (Luccini et al. 2007), and spinal cord (Lu et al. 2005). We did not obtain any evidence for the presence of functional presynaptic NMDA receptors in this study, suggesting that such receptors might not be located presynaptically on neurons that project to the PPN.

The decrease in frequency of mEPSCs by KA can be interpreted by the presence of presynaptic inhibitory metabotropic KA receptors located on glutamatergic nerve terminals. Alternatively, it is possible that bath application of KA may lead to desensitization of these receptors and subsequent decrease in the amplitude of mEPSCs, which may become undetectable if their amplitudes fall within the noise level. The increase in sEPSC frequency by NMDA and the lack of effect of NMDA on mEPSCs indicate that NMDA activates presynaptic receptors located on the soma of excitatory interneurons and not on their nerve terminals. In this case, NMDA activates or increases the firing of excitatory interneurons leading to an enhanced release of glutamate from their synaptic terminals. Therefore, blocking action potential propagation by TTX is expected to prevent NMDA-induced increase in sEPSCs.

Significance. In humans, there is a developmental decrease in REM sleep that occurs from birth until the end of puberty (Roffwarg et al. 1966). A similar decrease occurs in the rat from postnatal *days 10* to *30* (Jouvet-Mounier et al. 1970), with the most significant changes occurring between 10 and 15 days (Garcia-Rill et al. 2008). The landmark study describing the developmental decrease in REM sleep in humans concluded "proof that the critical function of the REM sleep mechanism during development is one of 'auto-stimulation' of structural and responsive capacity in the central nervous system must await future experimentation" (Roffwarg et al. 1966). The present study provides some evidence for the Roffwarg et al. (1966) ontogenetic hypothesis of sleep.

Changes in waking and SWS also occur from birth until adulthood in humans. Time spent in waking increases from ~8 h in the newborn to 16 h in the adult, whereas SWS shows a much less substantial decline, decreasing from 8 h in the newborn to 5 h in the adult (Roffwarg et al. 1966). Therefore, the developmental increase of waking in humans appears to be at the cost of decreased REM sleep. Perhaps this is due to greater efficiency by areas, such as the PPN, to promote the waking state, with one possible mechanism being the generation of high-frequency, gamma-band activity by the PPN.

High-frequency, low-amplitude oscillations were observed in EEG recordings during waking and REM sleep (Steriade et al. 1991). These gamma-frequency (>20 Hz) oscillations were originally believed to be present only in the cortex but recently have been recorded in other areas, such as the hippocampus (Whittington et al. 1997) and cerebellum (Middleton et al. 2008). The PPN is also capable of generating gamma-band activity (Simon et al. 2010), which may drive activity in higher areas such as the thalamus and the cortex. In population studies (recording local field potentials), differences in the frequency of activity induced by KA, NMDA, and CAR were observed. KA specifically induced low-frequency activity, CAR generated specific peaks of activity in the gamma range, whereas NMDA produced nonspecific peaks at gamma frequencies.

Gamma-band activity appears to be an intrinsic membrane property of PPN neurons, and it has been suggested that the mechanism behind this activity is the presence of high-threshold, voltage-dependent P/Q- and N-type calcium channels (Kezunovic et al. 2011). Other areas of the RAS, such as the Pf, generate gamma-band activity using the same mechanism as the PPN (Hyde et al. 2011). In contrast, other regions, such as the subcoeruleus nucleus, generate gamma-band activity through sodium-dependent subthreshold oscillations (Simon et al. 2011). Rather than via receptor regulation, the intrinsic "auto-stimulation" of the central nervous system proposed by the Roffwarg et al. (1966) ontogenetic hypothesis of REM sleep may be mediated by these voltage-dependent, intrinsic membrane properties. However, it has not yet been determined whether glutamate receptors interact with calcium channels to promote these intrinsic membrane properties.

It is possible that both the intrinsic membrane properties and the developmental changes in neurotransmitter actions and/or receptor number interact to produce the developmental decrease in REM sleep. Perhaps at young ages, a small, inward KA current, which increases REM sleep in the freely moving adult rat (Datta 2002), is sufficient to drive low-frequency oscillations and REM sleep. Another possibility is that interactions of multiple neurotransmitters may modulate the frequency of oscillations. For example, it is possible that activation of KA receptors in the young pup may produce only in a small oscillatory response, but coactivation of cholinergic receptors may drive the oscillations to higher amplitude and frequency, thus producing REM sleep.

Limitations. There are several limitations in this study that should be acknowledged. KA is a nonspecific agonist for KA receptors, and the antagonist CNQX blocks both KA and AMPA receptors (Bettler and Mulle 1995). It is likely that some of the recorded responses were due to activation of AMPA receptors as well as KA receptors, but, because these

do not appear to regulate sleep-wake cycles (Datta et al. 2002), we directed our study to NMDA and KA receptors.

Efferent targets of the PPN include the raphe nuclei, locus coeruleus, hypothalamus, amygdala, and subcoeruleus nucleus (Datta et al. 1999; Saper and Loewy 1980). The rationale for investigating the differences in glutamatergic responsiveness between PPN thalamic-projecting and randomly recorded PPN neurons was founded on published studies that showed differences between cholinergic responses of thalamic-projecting and randomly recorded PPN neurons (Good et al. 2007; Ye et al. 2010). In future studies, it would be interesting to test the responses of PPN projection neurons to other targets, such as the subcoeruleus nucleus.

When the effects of glutamate receptor agonists on the PPR, sEPSCs, and mEPSCs were tested, NMDA and KA activated postsynaptic receptors, resulting in an inward current and a decrease in R_{in}. The change in R_{in} could by itself result in changes to the PPR, sEPSCs, or mEPSCs that were unrelated to activation of presynaptic receptors. However, this is unlikely to be the case because, following NMDA application, there was a similar decrease in R_{in} that was not associated with changes in the PPR or the frequency of mEPSCs. Furthermore, application of CAR changed the R_{in}, but when a G protein blocker was used to prevent the decrease in R_{in}, CAR still produced a change in PPR, mEPSCs, and sEPSCs (Ye et al. 2010). Therefore, we believe that the changes in the properties of EPSCs observed following KA were due to activation of presynaptic receptors and not to a shunting effect produced by a decrease in R_{in}. Nevertheless, we do not exclude the presence of some postsynaptic effects on EPSCs by exogenously applied KA. In fact, KA is expected to slightly compete with endogenously released glutamate on postsynaptic AMPA/KA receptors, which may exhibit slight desensitization by bath-applied KA.

The present study tested the effects of NMDA and KA on EPSCs while blocking IPSCs using antagonists of $GABA_A$ and glycine receptors. NMDA or KA may activate GABAergic and/or glycinergic presynaptic neurons, increasing sIPSCs under normal conditions. Furthermore, presynaptic NMDA or KA receptors may be present on GABAergic and/or glycinergic terminals, but these experiments were beyond the scope of this study.

Conclusion. All PPN cells, regardless of cell type, respond to ionotropic glutamate receptor agonists. Developmental changes in the functional role of KA and NMDA receptors in excitatory synaptic transmission may underlie the changes in REM sleep that occur in the rat during this period. We also provide evidence for functional presynaptic glutamate receptors in the PPN, which may modulate the release of excitatory neurotransmitters.

ACKNOWLEDGMENTS

We thank Dr. Francisco Urbano for enthusiastic and constructive comments.

GRANTS

This work was supported by NIH Grant R01-NS-020246. Core facilities of the Center for Translational Neuroscience were supported by NIH Grant P20-RR-020146.

DISCLOSURES

No conflicts of interest, financial or otherwise, are declared by the author(s).

REFERENCES

Ben-Ari Y, Khazipov R, Leinekugel X, Caillard O, Gaiarsa JL. GABAA, NMDA and AMPA receptors: a developmentally regulated 'ménage à trois'. *Trends Neurosci* 20: 523–529, 1997.

Bettler B, Mulle C. Review: neurotransmitter receptors. II. AMPA and kainate receptors. *Neuropharmacology* 34: 123–139, 1995.

Campbell SL, Mathew SS, Hablitz JJ. Pre- and postsynaptic effects of kainate on layer II/III pyramidal cells in rat neocortex. *Neuropharmacology* 53: 37–47, 2007.

Capozzo A, Florio T, Cellini R, Moriconi U, Scarnati E. The pedunculopontine nucleus projection to the parafascicular nucleus of the thalamus: an electrophysiological investigation in the rat. *J Neural Transm* 110: 733–747, 2003.

Cathala L, Misra C, Cull-Candy S. Developmental profile of the changing properties of NMDA receptors at cerebellar mossy fiber-granule cell synapses. *J Neurosci* 20: 5899–5905, 2000.

Datta S. Evidence that REM sleep is controlled by the activation of brain stem pedunculopontine tegmental kainate receptor. *J Neurophysiol* 87: 1790–1798, 2002.

Datta S, Patterson EH, Siwek DF. Brainstem afferents of the cholinoceptive pontine wave generation sites in the rat. *Sleep Res Online* 2: 79–82, 1999.

Datta S, Patterson EH, Spoley EE. Excitation of the pedunculopontine tegmental NMDA receptors induces wakefulness and cortical activation in the rat. *J Neurosci Res* 66: 109–116, 2001a.

Datta S, Siwek DF. Single cell activity patterns of pedunculopontine tegmentum neurons across the sleep-wake cycle in the freely moving rats. *J Neurosci Res* 70: 611–621, 2002.

Datta S, Spoley EE, Mavanji VK, Patterson EH. A novel role of pedunculopontine tegmental kainate receptors: a mechanism of rapid eye movement sleep generation in the rat. *Neuroscience* 114: 157–164, 2002.

Datta S, Spoley EE, Patterson EH. Microinjection of glutamate into the pedunculopontine tegmentum induces REM sleep and wakefulness in the rat. *Am J Physiol Regul Integr Comp Physiol* 280: R752–R759, 2001b.

Debanne D, Guerineau NC, Gahwiler BH, Thompson SM. Paired-pulse facilitation and depression at unitary synapses in rat hippocampus: quantal fluctuation affects subsequent release. *J Physiol* 491: 163–176, 1996.

Delaney AJ, Jahr CE. Kainate receptors differentially regulate release at two parallel fiber synapses. *Neuron* 36: 475–482, 2002.

Garcia-Rill E, Charlesworth A, Heister D, Ye M, Hayar A. The developmental decrease in REM sleep: the role of transmitters and electrical coupling. *Sleep* 31: 673–690, 2008.

Good CH, Bay KD, Buchanan R, Skinner RD, Garcia-Rill E. Muscarinic and nicotinic responses in the developing pedunculopontine nucleus (PPN). *Brain Res* 1129: 147–155, 2007.

Heister DS, Hayar A, Garcia-Rill E. Cholinergic modulation of GABAergic and glutamatergic transmission in the dorsal subcoeruleus: mechanisms for REM sleep control. *Sleep* 32: 1135–1147, 2009.

Hille B. *Ion Channels of Excitable Membranes*. Sunderland, MA: Sinauer, 2001.

Hyde J, Kezunovic N, Simon C, Urbano FJ, Garcia-Rill E. Mechanism behind gamma band single cell activity in the parafascicular nucleus. *Association of Professional Sleep Societies, Minneapolis, MN, June 2011.*

Isaac JT, Crair MC, Nicoll RA, Malenka RC. Silent synapses during development of thalamocortical inputs. *Neuron* 18: 269–280, 1997.

Jin XT, Paré JF, Raju DV, Smith Y. Localization and function of pre- and postsynaptic kainate receptors in the rat globus pallidus. *Eur J Neurosci* 23: 374–386, 2006.

Jouvet-Mounier D, Astic L, Lacote D. Ontogenesis of the states of sleep in rat, cat, and guinea pig during the first postnatal month. *Dev Psychobiol* 2: 216–239, 1970.

Kamondi A, Williams JA, Hutcheon B, Reiner PB. Membrane properties of mesopontine cholinergic neurons studied with the whole-cell patch-clamp technique: implications for behavioral state control. *J Neurophysiol* 68: 1359–1372, 1992.

Kerchner GA, Wilding TJ, Li P, Zhuo M, Huettner JE. Presynaptic kainate receptors regulate spinal sensory transmission. *J Neurosci* 21: 59–66, 2001.

Kew JN, Richards JG, Mutel V, Kemp JA. Developmental changes in NMDA receptor glycine affinity and ifenprodil sensitivity reveal three distinct populations of NMDA receptors in individual rat cortical neurons. *J Neurosci* 18: 1935–1943, 1998.

Kezunovic N, Simon C, Hyde J, Smith K, Urbano FJ, Garcia-Rill E. Mechanism behind gamma band activity in the pedunculopontine nucleus. *Association of Professional Sleep Societies, Minneapolis, MN, June 2011*.

Kobayashi T, Good C, Biedermann J, Barnes C, Skinner RD, Garcia-Rill E. Developmental changes in pedunculopontine nucleus (PPN) neurons. *J Neurophysiol* 91: 1470–1481, 2004a.

Kobayashi T, Skinner RD, Garcia-Rill E. Developmental decrease in REM sleep: the shift to kainate receptor regulation. *Thalamus Relat Syst* 2: 315–324, 2004b.

Lauri SE, Segerstrale M, Vesikansa A, Maingret F, Mulle C, Collingridge GL, Isaac JT, Taira T. Endogenous activation of kainate receptors regulates glutamate release and network activity in the developing hippocampus. *J Neurosci* 25: 4473–4484, 2005.

Leonard CS, Llinas RR. Electrophysiology of mammalian pedunculopontine and laterodorsal tegmental neurons in vitro: implications for the control of REM sleep. In: *Brain Cholinergic Systems*, edited by Steriade M and Biesold D. New York: Oxford Science Publications, 1990, p. 205–223.

Li YH, Han TZ, Meng K. Tonic facilitation of glutamate release by glycine binding sites on presynaptic NR2B-containing NMDA autoreceptors in the rat visual cortex. *Neurosci Lett* 432: 212–216, 2008.

Llinas R, Ribary U. Consciousness and the brain. The thalamocortical dialogue in health and disease. *Ann NY Acad Sci* 929: 166–175, 2001.

Lu CR, Willcockson HH, Phend KD, Lucifora S, Darstein M, Valtschanoff JG, Rustioni A. Ionotropic glutamate receptors are expressed in GABAergic terminals in the rat superficial dorsal horn. *J Comp Neurol* 486: 169–178, 2005.

Luccini E, Musante V, Neri E, Raiteri M, Pittaluga A. *N*-methyl-D-aspartate autoreceptors respond to low and high agonist concentrations by facilitating, respectively, exocytosis and carrier-mediated release of glutamate in rat hippocampus. *J Neurosci Res* 85: 3657–3665, 2007.

Middleton SJ, Racca C, Cunningham MO, Traub RD, Monyer H, Knopfel T, Schofield IS, Jenkins A, Whittington MA. High-frequency network oscillations in cerebellar cortex. *Neuron* 58: 763–774, 2008.

Pickard L, Noel J, Henley JM, Collingridge GL, Molnar E. Developmental changes in synaptic AMPA and NMDA receptor distribution and AMPA receptor subunit composition in living hippocampal neurons. *J Neurosci* 20: 7922–7931, 2000.

Ramoa AS, McCormick DA. Enhanced activation of NMDA receptor responses at the immature retinogeniculate synapse. *J Neurosci* 14: 2098–2105, 1994.

Rodriguez-Moreno A, Sihra TS. Metabotropic actions of kainate receptors in the CNS. *J Neurochem* 103: 2121–2135, 2007.

Roffwarg HP, Muzio JN, Dement WC. Ontogenetic development of the human sleep-dream cycle. *Science* 152: 604–619, 1966.

Saper CB, Loewy AD. Efferent connections of the parabrachial nucleus in the rat. *Brain Res* 197: 291–317, 1980.

Schmitz D, Mellor J, Nicoll RA. Presynaptic kainate receptor mediation of frequency facilitation at hippocampal mossy fiber synapses. *Science* 291: 1972–1976, 2001.

Semba K, Fibiger HC. Afferent connections of the laterodorsal and the pedunculopontine tegmental nuclei in the rat: a retro- and antero-grade transport and immunohistochemical study. *J Comp Neurol* 323: 387–410, 1992.

Simon C, Kezunovic N, Urbano FJ, Garcia-Rill E. Gamma band sodium-dependent subthreshold oscillations in the subcoeruleus nucleus. *Association of Professional Sleep Societies, Minneapolis, MN, June 2011*.

Simon C, Kezunovic N, Ye M, Hyde J, Hayar A, Williams DK, Garcia-Rill E. Gamma band unit activity and population responses in the pedunculopontine nucleus. *J Neurophysiol* 104: 463–474, 2010.

Steinert JR, Postlethwaite M, Jordan MD, Chernova T, Robinson SW, Forsythe ID. NMDAR-mediated EPSCs are maintained and accelerate in time course during maturation of mouse and rat auditory brainstem in vitro. *J Physiol* 588: 447–463, 2010.

Steriade M, Datta S, Paré D, Oakson G, Curró Dossi RC. Neuronal activities in brain-stem cholinergic nuclei related to tonic activation processes in thalamocortical systems. *J Neurosci* 10: 2541–2559, 1990.

Steriade M, Dossi RC, Paré D, Oakson G. Fast oscillations (20–40 Hz) in thalamocortical systems and their potentiation by mesopontine cholinergic nuclei in the cat. *Proc Natl Acad Sci USA* 88: 4396–4400, 1991.

Steriade M, McCarley RW. *Brainstem Control of Wakefulness and Sleep*. New York: Plenum Press, 1990.

Takakusaki K, Kitai ST. Ionic mechanisms involved in the spontaneous firing of tegmental pedunculopontine nucleus neurons of the rat. *Neuroscience* 78: 771–794, 1997.

Van der Werf YD, Witter MP, Groenewegen HJ. The intralaminar and midline nuclei of the thalamus. Anatomical and functional evidence for participation in processes of arousal and awareness. *Brain Res Brain Res Rev* 39: 107–140, 2002.

Von Bohlen und Halbach O, Dermietzel R. *Neurotransmitters and Neuromodulators*. Weinheim, Germany: Wiley-VCH, 2006.

Wang HL, Morales M. Pedunculopontine and laterodorsal tegmental nuclei contain distinct populations of cholinergic, glutamatergic and GABAergic neurons in the rat. *Eur J Neurosci* 29: 340–358, 2009.

Whittington MA, Stanford IM, Colling SB, Jefferys JG, Traub RD. Spatiotemporal patterns of gamma frequency oscillations tetanically induced in the rat hippocampal slice. *J Physiol* 502: 591–607, 1997.

Ye M, Hayar A, Strotman B, Garcia-Rill E. Cholinergic modulation of fast inhibitory and excitatory transmission to pedunculopontine thalamic projecting neurons. *J Neurophysiol* 103: 2417–2432, 2010.